



RESEARCH ARTICLE | APRIL 01 2022

Fully coupled modeling of two-phase fluid flow and geomechanics in ultra-deep natural gas reservoirs

Weijun Shen (沈伟军) ; Tianran Ma (马天然); Xizhe Li (李熙喆) ; ... et. al



Physics of Fluids 34, 043101 (2022)

<https://doi.org/10.1063/5.0084975>



View
Online



Export
Citation

CrossMark

Articles You May Be Interested In

The geomechanical strength of carbonate rock in Kinta valley, Ipoh, Perak Malaysia

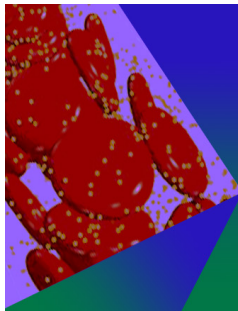
AIP Conference Proceedings (April 2018)

3D geomechanical modeling driven by acoustic impedance and seismic velocity: A case study of carbonate reservoir, East Java Basin

AIP Conference Proceedings (October 2018)

Geomechanical modeling of reservoir rock using 2D seismic inversion: Its application to wellbore stability in the onshore of Northwest Java Basin, Indonesia

AIP Conference Proceedings (October 2018)



Physics of Fluids

Special Topic: Flow and Forensics

Submit Today!

 AIP
Publishing

 AIP
Publishing

Fully coupled modeling of two-phase fluid flow and geomechanics in ultra-deep natural gas reservoirs

Cite as: Phys. Fluids **34**, 043101 (2022); doi: 10.1063/5.0084975

Submitted: 11 January 2022 · Accepted: 10 March 2022 ·

Published Online: 1 April 2022



View Online



Export Citation



CrossMark

Weijun Shen (沈伟军),^{1,2,a)}  Tianran Ma (马天然),³ Xizhe Li (李熙喆),^{4,a)} Baojiang Sun (孙宝江),⁵ Yong Hu (胡勇),⁴ and Jianchun Xu (徐建春)⁵

AFFILIATIONS

¹Key Laboratory for Mechanics in Fluid Solid Coupling Systems, Institute of Mechanics, Chinese Academy of Sciences, Beijing 100190, China

²School of Engineering Science, University of Chinese Academy of Sciences, Beijing 100049, China

³School of Mechanics and Civil Engineering, China University of Mining and Technology, Xuzhou, Jiangsu 221116, China

⁴PetroChina Research Institute of Petroleum Exploration and Development, Beijing 10083, China

⁵School of Petroleum Engineering, China University of Petroleum (East China), Qingdao 266580, China

^{a)}Authors to whom correspondence should be addressed: wjshen763@imech.ac.cn and lxz69@petrochina.com.cn

ABSTRACT

Efficiently and accurately understanding the fluid flow behavior in ultra-deep natural gas reservoirs is very challenging due to the complex geological environment and the intricate gas properties at high pressure. In this study, a fully coupled fluid flow and geomechanical model was developed to simulate complex production phenomena in ultra-deep natural gas reservoirs. Stress-dependent porosity and permeability models were applied, and then the governing equations of the model were incorporated into COMSOL Multiphysics. Furthermore, the model was verified by the reservoir depletion from the Keshen gas field in China, and the effects of reservoir properties and geomechanics on gas production were discussed. The results showed that the reservoir pressure and water saturation exhibited a significant funnel-shaped decline during the reservoir depletion. The higher relative permeability of the gas phase results in more methane gas production, thereby reducing the average pore pressure and gas saturation near the wellhead. When considering geomechanical effects, the production behavior significantly changes. The predictive value of gas production was higher when the reservoir rock deformation was ignored. The gas production exhibited strong positive correlations with reservoir porosity, fracture permeability, elastic modulus, and Poisson's ratio. Larger porosity, elastic modulus, and Poisson's ratio resulted in smaller deformation, while a smaller fracture permeability leads to larger deformation in ultra-deep natural gas reservoirs.

Published under an exclusive license by AIP Publishing. <https://doi.org/10.1063/5.0084975>

I. INTRODUCTION

With the advances in geological theory and exploration practices of global oil and gas, hydrocarbon exploration and development can be categorized into three major fields: onshore deep and ultra-deep, offshore deep water, and unconventional oil and gas. The new reserves and production of global deep and ultra-deep oil and gas show a trend of rapid growth.^{1,2} In recent years, a series of important discoveries have occurred in the field of ultra-deep oil and gas exploration in China. The exploration and development of ultra-deep natural gas resources (with a burial depth >6000 m) have been increasingly researched.^{3,4} According to the fourth oil/gas resource evaluation,

the total volume of conventional natural gas resources in China is $41 \times 10^{12} \text{ m}^3$, 40.2% of which is ultra-deep natural gas.⁵ Ultra-deep natural gas resources in China are abundant and have huge development potential; these resources play an important role in conventional gas production growth and become a significant strategic field in the upstream business.⁶ Therefore, speeding up the exploration and development of ultra-deep natural gas resources is of great significance for the natural gas supply and for optimizing the energy structure in China.

Ultra-deep natural gas reservoirs are characterized by low-average porosity and permeability, high temperature, high pressure, high *in situ* stress, and strong plasticity in rocks. Complex fluid flows

are characteristic of ultra-deep natural gas formations.^{7,8} During the depletion of ultra-deep natural gas reservoirs, the reservoir rock deformation caused by overburden pressure leads to remarkable changes in porosity and permeability. The coupling between fluid flow and *in situ* stress fields is strong and cannot be ignored.^{6,9} The coupled fluid flow and mechanical deformation in reservoir media play a significant role in subsurface hydrology and hydrocarbon recovery.¹⁰ Terzaghi¹¹ proposed the effective stress concept in saturated, deformable porous media. The research established a one-dimensional consolidation model and then extended it to a three-dimensional consolidation model. Based on the total stress and pore fluid pressure in saturated soils, Biot^{12,13} analyzed the interaction between three-dimensional deformed materials and pore pressure and developed a relatively perfect three-dimensional consolidation theory. Brooks and Corey¹⁴ and van Genuchten¹⁵ developed two well-known relative permeability models of water saturation in unconsolidated and consolidated porous media, respectively. Considering the nonlinearity of the geometry and material, Zienkiewicz and Shiomi¹⁶ put forward the generalized Biot formulation according to three-dimensional consolidation theory. To describe elastic mechanical deformation, Liu *et al.*¹⁷ developed a general stress–strain relationship in porous and fractured rock subject to elastic mechanical deformation. Moosavi *et al.*¹⁸ measured the deformation characteristics of pores at different effective stresses and derived relationships of porosity and permeability with effective stress. Zheng *et al.*¹⁹ developed theoretical models for the essential relationships between porosity, permeability, and effective stresses in low-permeability sedimentary rock. Consequently, the theory and application of fluid–solid coupling interactions have advanced from one-dimensional consolidation to three-dimensional consolidation and from linear elasticity to nonlinear elasticity of rock deformation.

The problems of coupled fluid flow and geomechanics in reservoirs have been investigated by researchers in mining and geo-energy fields. Chin *et al.*²⁰ developed a coupled fluid flow and geomechanical model to analyze pressure-transient problems in hydrocarbon reservoirs with stress-dependent permeability for nonlinear elastic and plastic constitutive behavior. Gutierrez *et al.*²¹ discussed the issues related to the interaction between multiphase fluid flow and rock deformation in hydrocarbon reservoirs. Ambekar *et al.*¹⁰ developed a geomechanical model with modular coupling and elastoplastic rock behavior and then applied it to several field studies. Considering the strain and pressure depletion under uniaxial strain conditions, Shi and Durucan²² proposed stress-based permeability models in the producing reservoirs. Nair *et al.*²³ proposed a finite element (FE) model to simulate two-phase flow and solid deformation in a dual-porosity medium. Ma *et al.*²⁴ described the coupled process of two-phase flow and rock deformation caused by pore pressure and analyzed the geomechanical effects on gas production in the reservoir depletion. Liu *et al.*²⁵ reported a coupled multiphase flow and geomechanical model to analyze fracturing fluid recovery and distribution in fractured gas reservoirs. Sangnimmuan *et al.*²⁶ developed a coupled fluid flow and geomechanical model to understand stress evolution due to the reservoir depletion with complex fracture geometries. Despite many studies on coupled fluid flow and geomechanical behavior in geological reservoirs, research on coupled flow and mechanics *in situ* high-temperature, high-pressure, and high-stress conditions are still lacking. During the depletion of ultra-deep natural gas reservoirs, there is multiphase fluid flow and geomechanical responses due to the high-

temperature, high-pressure, and high *in situ* stress conditions. Hence, it is necessary to understand the coupled fluid flow and geomechanical behavior under these conditions so as to optimize extraction conditions and ultimately enhance gas production in ultra-deep natural gas reservoirs.

In this study, a coupled multiphase flow and geomechanical model was developed to describe the coupled process of permeability evolution and gas production in ultra-deep natural gas reservoirs. The stress-dependent porosity and permeability, as well as rock deformation induced by pore pressure, were considered in this model. The models were run using COMSOL Multiphysics. The validation model was from the study on the reservoir depletion from the Keshen gas field in China. Then, the two-phase fluid flow and reservoir effective stress were analyzed. Furthermore, the effects of reservoir properties on gas production and permeability evolution are discussed.

II. MATHEMATICAL MODELS

A. Fluid flow model

According to the law of conservation of mass, the fluid flow in the reservoir matrix can be expressed as follows:^{27,28}

$$\frac{\partial \phi_m \rho_\alpha}{\partial t} + \nabla \cdot (\rho_{m\alpha} \mathbf{u}_\alpha) = Q_{fm\alpha}, \quad (1)$$

where ϕ_m is the matrix porosity, ρ_α is the fluid density in the matrix ($\alpha = g$ for gas and $\alpha = w$ for water), t is the time, \mathbf{u}_α is the flow velocity in the matrix, and $Q_{fm\alpha}$ is the exchange term of the gas or water phase between the matrix and the fracture.

The exchange term of the gas and water phase can be written as follows:²⁹

$$Q_{fm\alpha} = 8 \left(1 + \frac{2}{s^2} \right) \frac{k_m k_{mr\alpha} \rho_{m\alpha}}{\mu_\alpha} (p_{m\alpha} - p_{f\alpha}), \quad (2)$$

where k_m is the matrix permeability, $k_{mr\alpha}$ is the relative permeability of fluids in the matrix, $\rho_{m\alpha}$ is the fluid density, s is the shape factor, μ_α is the fluid viscosity, and $p_{m\alpha}$ and $p_{f\alpha}$ are the pressures in the matrix and the fracture, respectively.

Substituting Eq. (2) into Eq. (1), the mass conservation equation for the fluid in the reservoir matrix can be written as

$$\frac{\partial \phi_m \rho_\alpha}{\partial t} + \nabla \cdot (\rho_{m\alpha} \mathbf{u}_\alpha) = 8 \left(1 + \frac{2}{s^2} \right) \frac{k_m k_{mr\alpha} \rho_{m\alpha}}{\mu_\alpha} (p_{m\alpha} - p_{f\alpha}). \quad (3)$$

Similarly, the mass conservation equation for two-phase flow in the reservoir fracture can be expressed as follows:

$$\frac{\partial \phi_f \rho_i}{\partial t} + \nabla \cdot (\rho_{fi} \mathbf{u}_i) = Q_i, \quad (4)$$

where ϕ_f is the fracture porosity, ρ_i is the density of the gas (water) phase in the fracture, t is the time, \mathbf{u}_i is the flow velocity of the gas (water) phase in the fracture, Q_i is the mass conservation of the gas (water) phase in the fracture, and the subscript i represents the phase ($i = g$ for gas and $i = w$ for water).

According to the assumption of the dual-permeability model, there are gas and water in both the fracture and the matrix system of the reservoir.^{30,31} Thus, Eq. (4) can be written as

$$\left\{ \begin{aligned} & \frac{\partial \varphi_f s_{fg} \rho_{fg}}{\partial t} - \nabla \cdot \left(\frac{\rho_{fg} k k_{rg}}{\mu_g} \nabla P_{fg} \right) \\ & = 8 \left(1 + \frac{2}{s^2} \right) \frac{k_m k_{mrg} \rho_{mg}}{\mu_g} (P_{mg} - P_{fg}), \\ & \frac{\partial \varphi_f s_{fw} \rho_{fw}}{\partial t} - \nabla \cdot \left(\frac{\rho_w k k_{rw}}{\mu_w} \nabla P_{fw} \right) \\ & = 8 \left(1 + \frac{2}{s^2} \right) \frac{k_m k_{mrw} \rho_{mw}}{\mu_w} (P_{mw} - P_{fw}). \end{aligned} \right. \quad (5)$$

During the reservoir depletion, the reservoir porosity depends on anisotropic elastoplastic properties, and the reservoir permeability is a function of the porosity changes and effective normal stress. The stress-dependent porosity and permeability models were adopted and expressed as

$$\varphi_\beta = \alpha_\beta + (\varphi_{\beta 0} - \alpha_\beta) \exp\left(-\frac{\Delta\sigma'}{K}\right), \quad (6)$$

$$\frac{k_\beta}{k_0} = \left[\frac{\alpha_\beta + (\varphi_{\beta 0} - \alpha_\beta) \exp\left(-\frac{\Delta\sigma'}{K}\right)}{\varphi_{\beta 0}} \right]^3, \quad (7)$$

where φ_{f0} and k_0 are the initial porosity and permeability at reservoir initial stress, respectively; the subscript β represents the reservoir matrix or the fracture; α_β is the Biot coefficient; K is the drained bulk modulus; and σ' is the effective mean stress.

B. Geomechanical model

Based on the generalized Hooke's law, the governing equation for deforming reservoir rocks can be expressed as^{12,32}

$$\sigma_{ij} = \lambda \varepsilon_{kk} \delta_{ij} + 2G \varepsilon_{ij} - \alpha p_m \delta_{ij} - \beta p_f \delta_{ij}, \quad (8)$$

where σ_{ij} is the total rock stress; λ is the Lamé constant; ε_{kk} and ε_{ij} are the rock strain in the kk and ij directions, respectively; δ_{ij} is the Kronecker delta; G is the shear modulus; α and β are the Biot coefficients of the matrix and fracture, respectively; p_f is the fracture pressure ($p_f = s_{wf} P_{wf} + s_{gf} P_{gf}$); and p_m is the pore pressure ($p_m = s_{wm} P_{wm} + s_{gm} P_{gm}$).

Assuming that there are only small deformations occurring in the reservoir rocks,³³ the geometric equation can be expressed as

$$\varepsilon_{ij} = \frac{1}{2} (u_{i,j} + u_{j,i}), \quad (9)$$

where $u_{i,j}$ and $u_{j,i}$ are the displacement in the j and i directions, respectively.

According to the porous elastic theory,³⁴ the equilibrium equation of reservoir rocks without consideration of the inertia force mass can be expressed as

$$\sigma_{ij,j} + F_i = 0, \quad i = 1, 2, 3, \quad j = 1, 2, 3, \quad (10)$$

where F_i is the body force in the i direction.

Substituting Eqs. (8) and (9) into Eq. (10), the governing equation of the reservoir stress can be expressed as³⁵

$$G u_{i,kk} + \frac{G}{1-2\nu} u_{k,ki} - \alpha p_{m,i} - \beta p_{f,i} + F_i = 0. \quad (11)$$

In this study, Eqs. (3), (5), and (11) are the final governing equations of the fully coupled geomechanical model with two-phase fluid flow considering the stress-dependent porosity and permeability induced by pore pressure in ultra-deep gas reservoirs. The above three equations are incorporated into the partial differential equation and the solid mechanics modules of COMSOL Multiphysics, which solves equations using the FE method.

III. NUMERICAL MODELING

To understand the coupled fluid flow and geomechanical behavior in ultra-deep natural gas reservoirs, the reservoir depletion from the Keshen gas field in China was considered in this study. The Keshen gas field is located in the Kelasu structural belt of the Tarim Basin in China, which is one of the vast gas fields in Northwest China.³⁶ The target layer is the Bashijiqike Formation of the Cretaceous, with pressure coefficients exceeding 1.5. The burial depth is 5500–7500 m, and the temperature is 160–180 °C, which is within the ultra-deep and ultra-high pressure gas reservoirs.³⁷ The gas reservoirs are mainly lithic feldspar sandstone with a matrix porosity of less than 10% and the matrix permeability generally below 0.1 mD. The reservoir fractures are highly developed, and high-angle and reticulate fractures are dominant. The fracture permeability is approximately 200 mD. Based on the geological characteristics of the reservoirs in the Keshen gas field, COMSOL Multiphysics was used to construct and solve the numerical reservoir model with dimensions of 1800 m (length) × 1800 m (width) × 300 m (height) as shown in Fig. 1.

Table I summarizes the detailed reservoir and fracture properties used in the simulation. The reservoir is considered a dual permeability

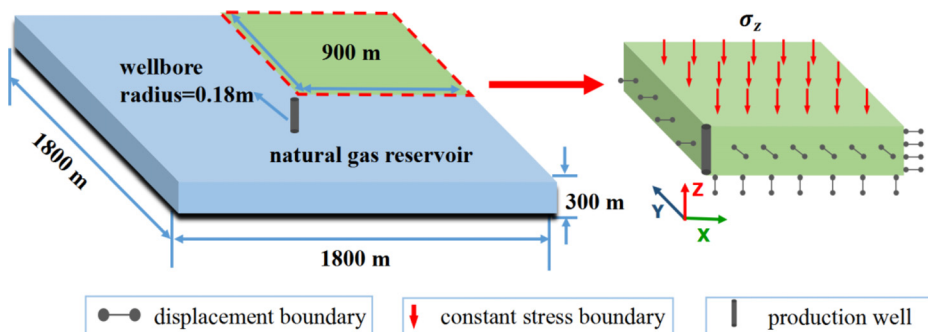


FIG. 1. Sketch of the geometric model and boundary conditions for simulating the reservoir production.

TABLE I. Reservoir properties and parameters used in the simulation.

Parameters	Value	Parameters	Value
Drainage	$1800 \times 1800 \text{ m}^2$	Biot coefficient	1
Reservoir thickness	300 m	Initial reservoir pressure	100 MPa
Reservoir depth	6500 m	Initial water saturation	0.3874
Rock density	2600 kg/m^3	Wellhead pressure	74 MPa
Poisson's ratio of rock	0.3	Water viscosity	$5.5 \times 10^{-5} \text{ Pa s}$
Elastic modulus of rock	20 GPa	Gas viscosity	$4.74 \times 10^{-5} \text{ Pa s}$
Matrix porosity	0.05	Initial water density	1000 kg/m^3
Matrix permeability	0.1 mD	Initial methane density	0.684 kg/m^3
Fracture porosity	0.01	Water compressibility	$1.52 \times 10^{-7} \text{ Pa}^{-1}$
Fracture permeability	200 mD	Methane compressibility	$4.08 \times 10^{-11} \text{ Pa}^{-1}$

model, including reservoir matrix and reservoir fracture. In this study, the water and gas flow in the reservoir matrix and reservoir fracture are described with two different sets of relative permeability curves based on the experimental results, as illustrated in Fig. 2(a).³⁸ The capillary pressure curve used in the reservoir matrix is presented in Fig. 2(b), while the capillary pressure in the reservoir fracture is assumed to be zero because of the larger permeability in the fracture.

IV. RESULTS AND DISCUSSION

A. Model validation and production characteristics

Based on the above mathematical models, the gas reservoir was simulated with COMSOL Multiphysics. The comparison between the simulation result and field data is shown in Fig. 3. With the depletion of the gas reservoir, the daily gas production gradually decreased until certain abandonment conditions and the production well was closed. The simulation result was essentially in agreement with the field data, and it implied that the models reflect the flow characteristics of ultra-deep reservoirs. Thus, the models were used to analyze and predict the production performance. Figures 4, 5, and 6 illustrate the spatial distribution of reservoir pore pressure, reservoir water saturation, and reservoir effective stress, respectively. From these figures, the reservoir

pressure and water saturation showed a significant funnel-shaped decline from the far field of the reservoir to the wellhead. During the reservoir depletion, the relative permeability of the gas phase was high. This condition resulted in an increase in methane gas production, which reduced the average pore pressure and gas saturation near the wellhead. Due to the continuous decrease of the displacement boundary constraint at the wellhead and the pore pressure, stress changes were evident. Consequently, further detection near the wellhead should be required to prevent the damage or fractures during the gas reservoir development. Based on Fig. 3, the daily gas production in the latter period was much lower than that in the initial stage, which indicated that the depletion effect reached a farther boundary.

The evolution of pore pressure, water saturation, and effective stress at monitoring points P1 (5, 5, 150) and P2 (50, 50, 150) is illustrated in Fig. 7. As gas and water are depleted in the gas reservoir, the reservoir pressure began to decrease and the pore pressure at P1 clearly and rapidly decreased. The water saturation curve decreased and then increased over a short time, mainly because the higher relative permeability in the initial gas phase encouraged more gas to migrate from the far field to the wellhead. With a decrease of the pore pressure, the average effective stress at P1 and P2 increased.

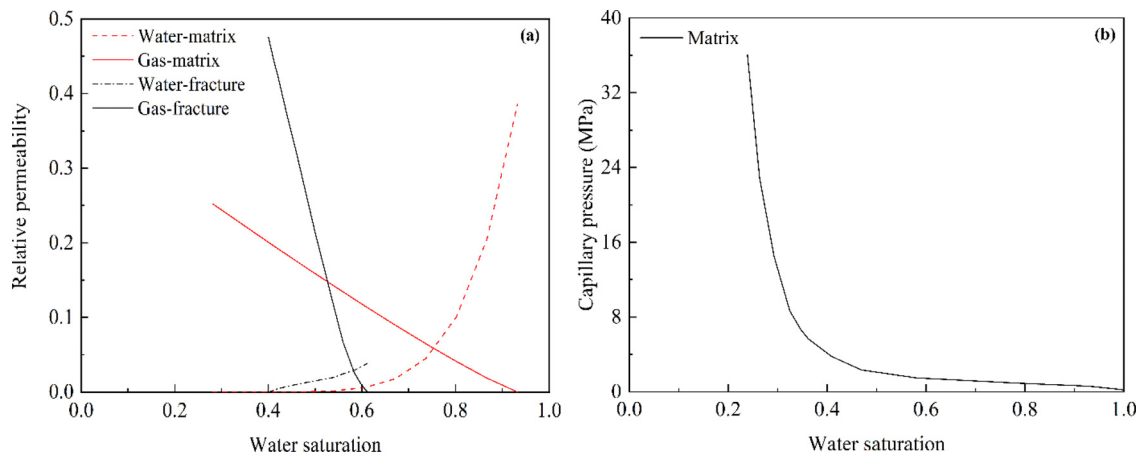


FIG. 2. (a) Two different sets of relative permeability curves for the reservoir matrix and fracture; (b) capillary pressure for matrix.

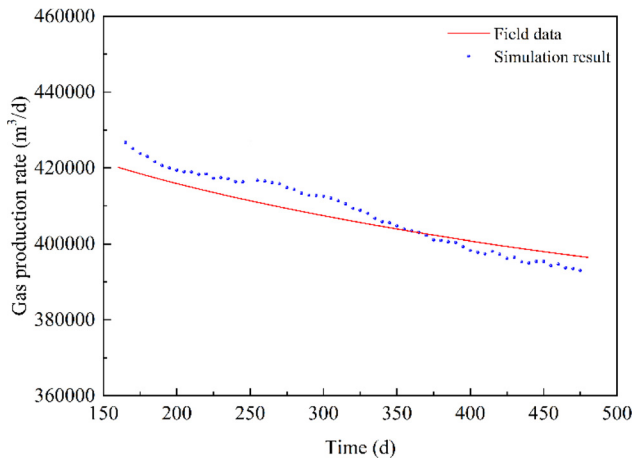


FIG. 3. Comparison between simulation results and field data.

B. Effects of the reservoir porosity

The reservoir porosity is an important attribute for evaluating reservoir quality and calculating reservoir reserves as it reflects the storage capacity of reservoir rocks.^{39,40} The effects of the reservoir porosity from 1% to 10% are selected to understand gas production and permeability evolution in this study. Figure 8 illustrates the

evolution of gas production and the permeability ratio under various porosity changes. Based on Fig. 8, a larger reservoir porosity corresponds to a greater gas production ratio. A larger porosity provides more storage space for gas. Consequently, a larger porosity of the reservoir leads to higher gas production. For gas reservoirs with different porosities, the reservoir with a smaller porosity is more prone to pressure reductions, which are most obvious in the later stages of exploitation. According to the cubic law of permeability, the permeability will decrease sharply, and it will affect the gas production rate in the later stages.

C. Effects of the fracture permeability

Permeability is one of the most important reservoir seepage characteristics, especially for gas productivity forecasting, which controls the gas-flow capacity and production deliverability in reservoirs.^{41,42} A larger permeability means there is a higher fracture density or wider spacing in reservoirs, which provides more rapid flow space for gas and water. Fracture permeability values between 120 and 200 mD are used to investigate gas production and permeability changes in reservoirs. The trends of gas production and the permeability ratio under various fracture permeability conditions are shown in Fig. 9. According to Fig. 9(a), a greater reservoir fracture permeability correlates with a greater gas production rate. The reservoir fracture permeability decreases rapidly over a short time due to the rapid decrease of pressure at the initial stage of exploitation [Fig. 9(b)]. A lower reservoir

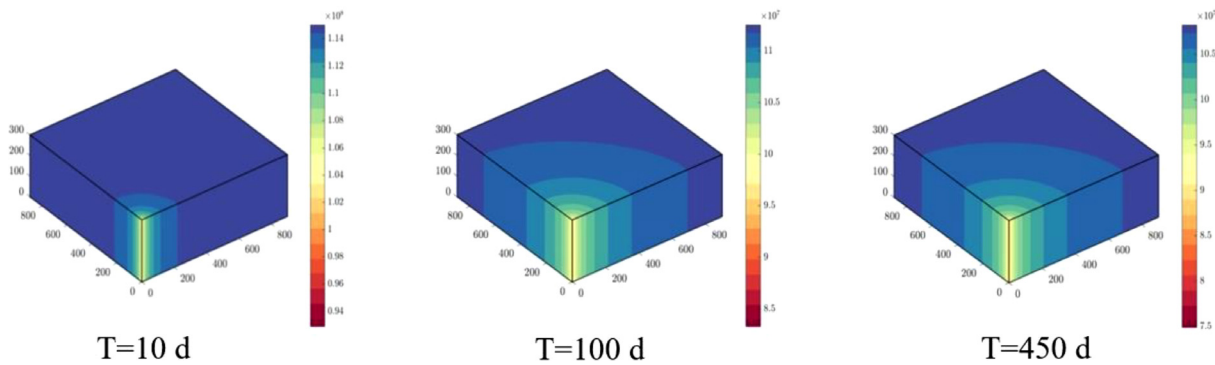


FIG. 4. Spatial distribution of reservoir pore pressure.

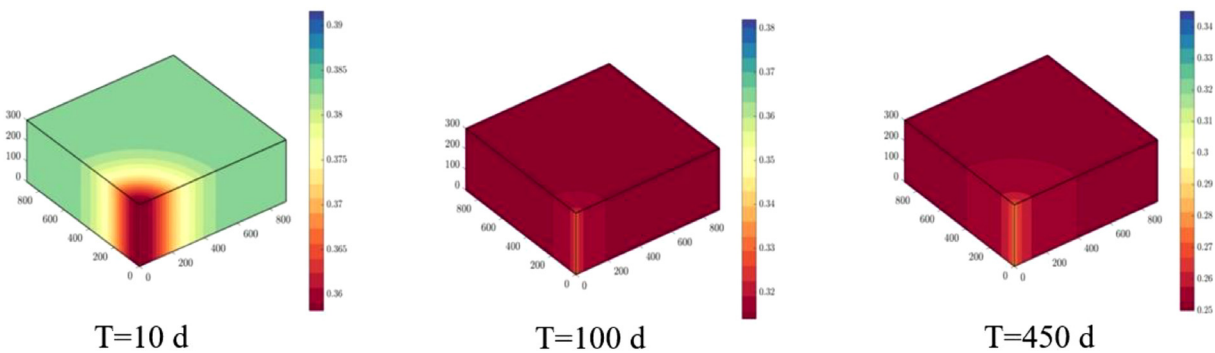


FIG. 5. Spatial distribution of reservoir water saturation.

Downloaded from http://pubs.aip.org/aip/pof/article-pdf/doi/10.1063/5.0084975/16604284/043101_1_online.pdf

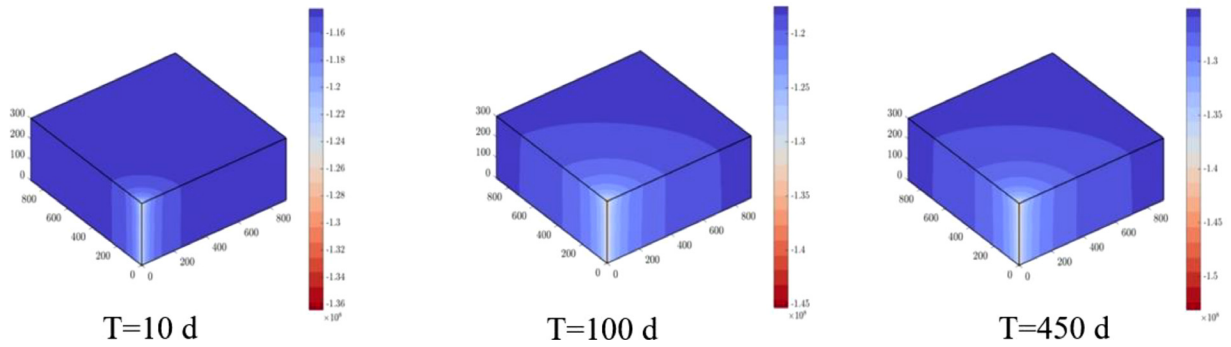


FIG. 6. Spatial distribution of reservoir effective stress.

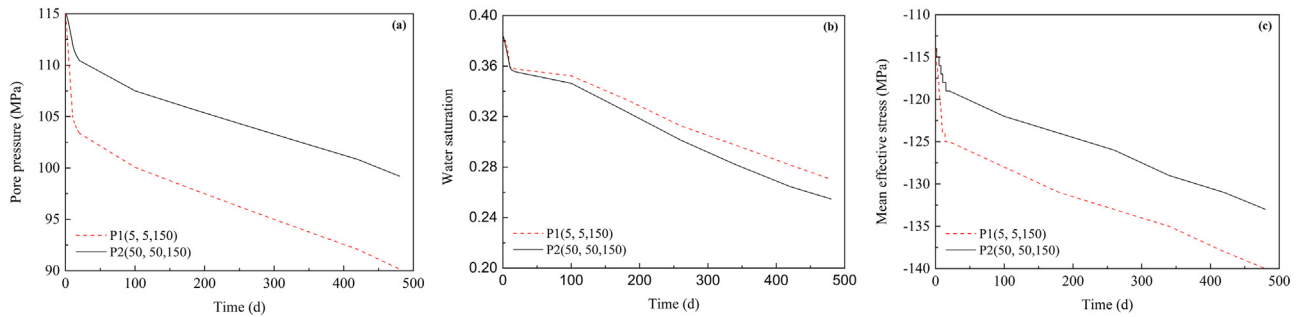


FIG. 7. Evolution of reservoir pore pressure (a), water saturation (b), and mean effective stress (c) in P1 and P2.

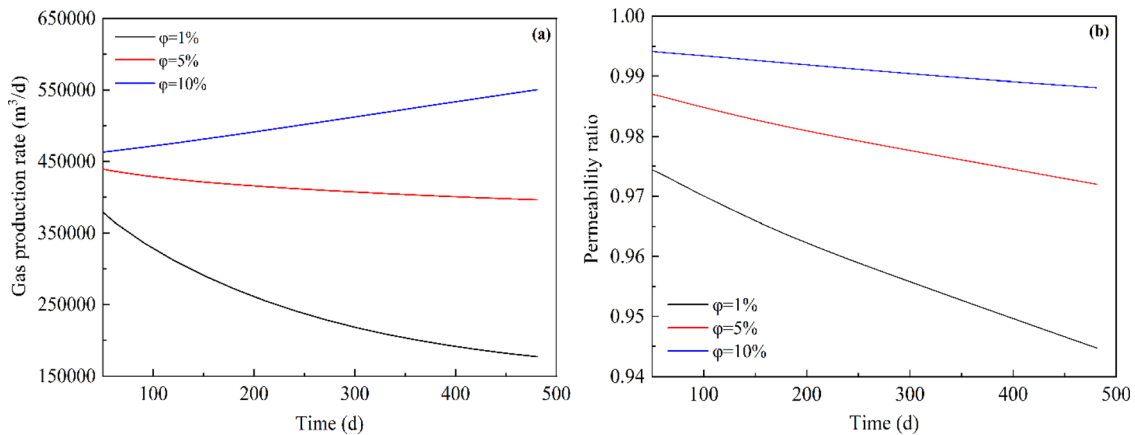


FIG. 8. Evolution of gas production (a) and permeability ratio (b) under various porosity models.

fracture permeability delays the decrease of reservoir fracture permeability because a lower pressure and smaller change of effective stress lead to a smaller effect of the fracture permeability. Therefore, a greater reservoir fracture permeability results in a faster and wider-ranging decrease.

D. Effects of coupled and uncoupled models

During the depletion of gas reservoirs, when the reservoir pore pressure gradually decreases, the effective stress will change.⁴³ In this study, the influences of reservoir rock deformation on gas production and permeability evolution were determined in ultra-deep natural gas

Downloaded from http://pubs.aip.org/phf/article-pdf/doi/10.1063/5.0084975/16604284/043101_1_online.pdf

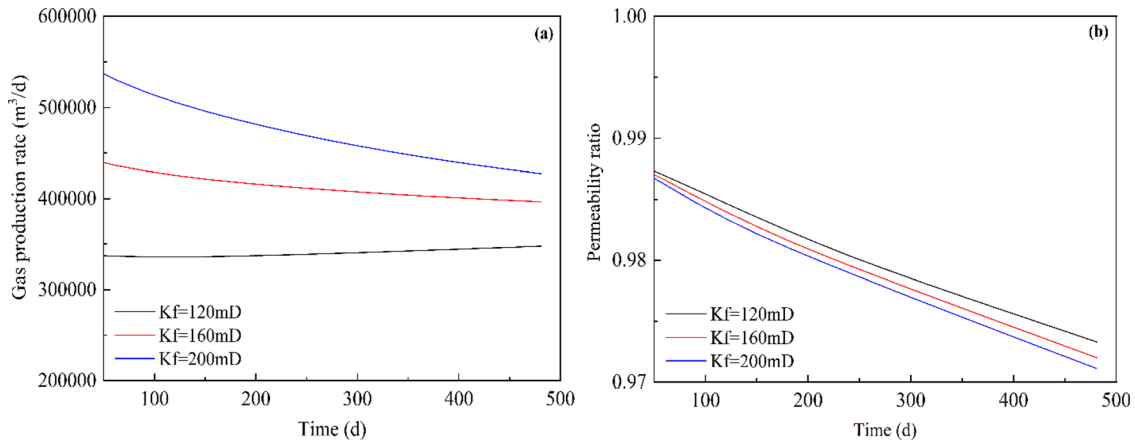


FIG. 9. Evolution of gas production (a) and permeability ratio (b) under various permeability models.

reservoirs. Figure 10 illustrates the evolution of gas production and permeability under the coupled and uncoupled models. According to Fig. 10(a), the gas production curves in the coupled and uncoupled models show similar trends. During the early stage of the reservoir depletion, the gas in the ultra-deep natural gas reservoir will flow from high-pressure storage formation to the wellhead due to the pressure gradient. With such a large pressure gradient, the reservoir gas continuously flows to the ground and then rapidly reaches the peak. With a decrease of reservoir pressure, the extent of gas production accordingly decreases. With a decrease of pore pressure and increase of effective stress in the exploitation process, the fracture channel is effectively compressed and results in the reduction of the permeability ratio, as illustrated in Fig. 10(b). If the effect of reservoir rock deformation during the reservoir depletion is ignored, then the predictive value of gas production will be higher, which will affect the evaluation of production wells.

E. Effects of Young’s modulus

The elastic modulus describes the linear elastic deformation response of rock under the deformation condition, which is an

important geo-mechanical parameter used for defining the phenomena in rock mass.⁴⁴ The evolution of gas production and the permeability ratio under different elastic moduli are illustrated in Fig. 11. With an increase of the elastic modulus, the gas production increases, and the increase of the elastic modulus will contribute to improving the gas production rate and maintaining the same trend. The elastic modulus of the fractures in reservoir rocks increases with an increase of the elastic modulus, which results in compressibility reduction. Under the same effective stress condition, the deformation of reservoir fractures and ultimately the permeability are reduced. When the elastic modulus goes to infinity, the predicted flow rate is consistent with that of the result without considering the deformation caused by pore pressure.

F. Effects of Poisson’s ratio

Poisson’s ratio of rocks is the negative of the ratio of transverse strain to axial strain when an isotropic rock is subjected to uniaxial stress only; this process is considered a significant mechanical property that can be used to predict geomechanical behavior during the

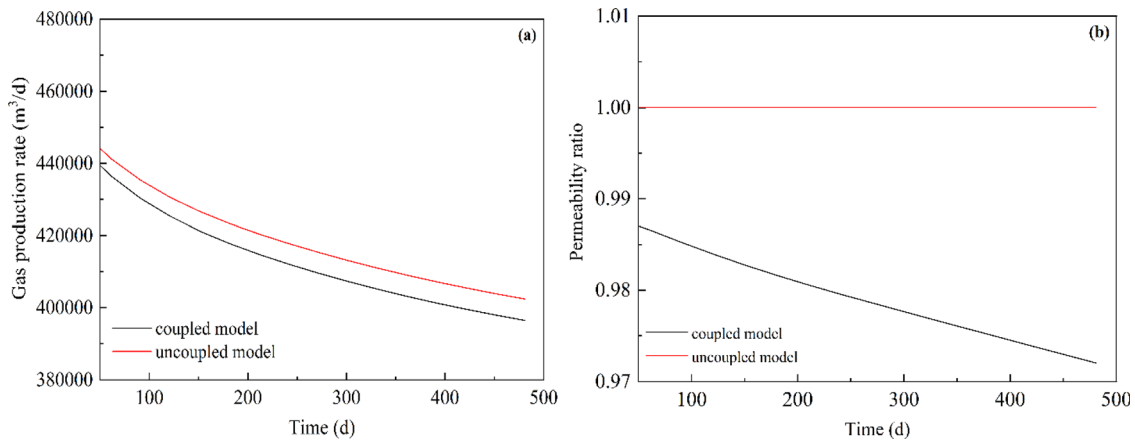


FIG. 10. Evolution of gas production (a) and permeability ratio (b) under coupled and uncoupled models.

Downloaded from http://pubs.aip.org/aip/pof/article-pdf/doi/10.1063/5.0084975/16604294/043101_1_online.pdf

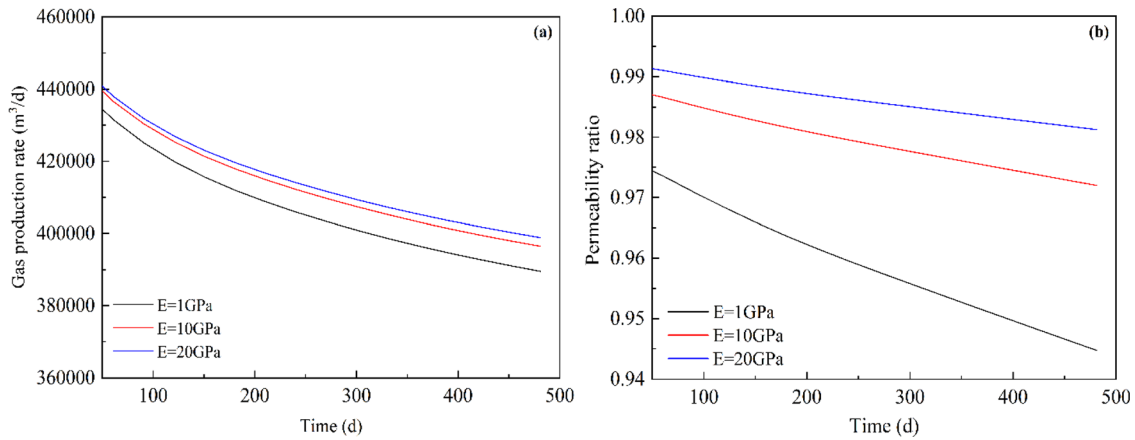


FIG. 11. Evolution of gas production (a) and the permeability ratio (b) under various elastic moduli.

reservoir depletion.⁴⁵ Poisson’s ratio is a dimensionless physical quantity used to reflect Poisson’s phenomenon. Poisson’s phenomenon describes the following: when a material is compressed in one direction, it will elongate in the other two directions perpendicular to that direction. The evolution of gas production and permeability under different Poisson’s ratio values is shown in Fig. 12. With an increase of Poisson’s ratio, the gas production increases; this condition is favorable for gas production, which maintains a consistent trend because an increase of Poisson’s ratio indicates that the reservoir is not easily deformed and that the compressibility of reservoir fractures is reduced. The compressibility of reservoirs with a high Poisson’s ratio decreases at the same effective stress condition while the gas production and permeability increase.

V. CONCLUSIONS

In this study, a mathematical model was developed to describe the coupled process of incorporating two-phase fluid flow and rock deformation caused by pore pressure during the reservoir depletion in ultra-deep natural gas reservoirs. Stress-dependent porosity and

permeability models were adopted in this model. Based on the FE method, the governing equations of the model were then implemented and solved in COMSOL Multiphysics. The model was verified by the reservoir depletion from the Keshen gas field in China, and the two-phase fluid flow behavior was analyzed. In addition, the influences of reservoir properties and geomechanics on gas production and permeability evolution were discussed. According to the above results, the following conclusions can be drawn: (1) During the reservoir depletion, the reservoir pressure and water saturation exhibited a significant funnel-shaped decline from the far field of the reservoir to the wellhead. The relative permeability of the gas phase was high, and it led to additional methane gas production. The result was a reduction of the average pore pressure and gas saturation near the wellhead. (2) The production behavior differed when considering the geomechanical effect in ultra-deep natural gas reservoirs. If the effect of reservoir rock deformation was ignored, then the predictive value of gas production was higher. This scenario affected the evaluation of production wells. (3) Reservoir porosity, fracture permeability, elastic modulus, and Poisson’s ratio directly influenced the gas production and rock

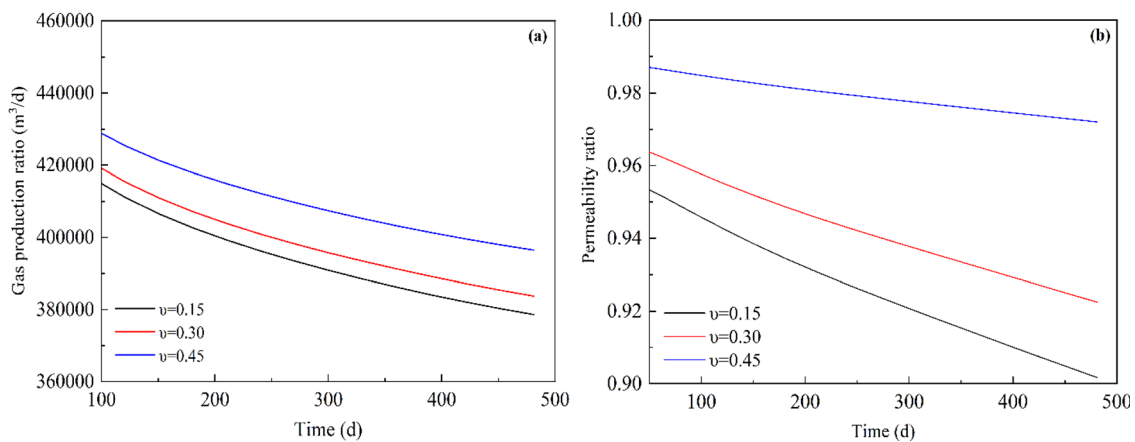


FIG. 12. Evolution of gas production (a) and permeability ratio (b) under various Poisson’s ratio values.

Downloaded from http://pubs.aip.org/aip/pof/article-pdf/doi/10.1063/5.0084975/16604294/043101_1_online.pdf

deformation. With an increase of reservoir porosity, fracture permeability, elastic modulus, and Poisson's ratio, the gas production increased in the reservoirs. Larger porosity, elastic modulus, and Poisson's ratio in ultra-deep natural gas reservoirs corresponded to a smaller deformation in the reservoirs. The smaller fracture permeability results in larger deformation of ultra-deep natural gas reservoirs.

ACKNOWLEDGMENTS

This work was supported by the National Natural Science Foundation of China (Grant Nos. U1762216, 12172362, and 11802312).

AUTHOR DECLARATIONS

Conflict of Interest

The authors have no conflicts to disclose.

DATA AVAILABILITY

The data that support the findings of this study are available from the corresponding authors upon reasonable request.

REFERENCES

- W. R. Hu, J. W. Bao, and B. Hu, "Trend and progress in global oil and gas exploration," *Pet. Explor. Dev.* **40**(4), 439 (2013).
- W. J. Shen, X. Z. Li, T. R. Ma *et al.*, "High-pressure methane adsorption behavior on deep shales: Experiments and modeling," *Phys. Fluids* **33**(3), 063103 (2021).
- C. Z. Zou, G. M. Zhai, G. Y. Zhang *et al.*, "Formation, distribution, potential and prediction of global conventional and unconventional hydrocarbon resources," *Pet. Explor. Dev.* **42**(1), 14 (2015).
- J. Z. Li, X. W. Tao, B. Bai *et al.*, "Geological conditions, reservoir evolution and favorable exploration directions of marine ultra-deep oil and gas in China," *Pet. Explor. Dev.* **48**(1), 60 (2021).
- Y. Gan, H. M. El-Houjeiri, A. Badahdah *et al.*, "Carbon footprint of global natural gas supplies to China," *Nat. Commun.* **11**, 824 (2020).
- X. Z. Li, Z. H. Guo, Y. Hu *et al.*, "High-quality development of ultra-deep large gas fields in China: Challenges, strategies and proposals," *Nat. Gas Ind.* **7**(5), 505 (2020).
- Y. Jin, K. P. Chen, M. Chen *et al.*, "Short-time pressure response during the startup of a constant-rate production of a high pressure gas well," *Phys. Fluids* **23**, 043101 (2011).
- C. H. Yang and J. J. Liu, "Petroleum rock mechanics: An area worthy of focus in geo-energy research," *Adv. Geo-Energy Res.* **5**(4), 351–352 (2021).
- D. X. Zhang, L. H. Zhang, H. Y. Tang *et al.*, "A novel fluid-solid coupling model for the oil-water flow in the natural fractured reservoirs," *Phys. Fluids* **33**(3), 036601 (2021).
- A. S. Ambekar, S. Mondal, and V. V. Buwa, "Pore-resolved volume-of-fluid simulations of two-phase flow in porous media: Pore-scale flow mechanisms and regime map," *Phys. Fluids* **33**(1), 102119 (2021).
- K. Terzaghi, *Theoretical Soil Mechanics* (Wiley, New York, 1943).
- M. A. Biot, "General theory of three dimensional consolidation," *J. Appl. Phys.* **12**(5), 155 (1941).
- M. A. Biot, "Mechanics of deformation and acoustic propagation in porous media," *J. Appl. Phys.* **33**, 1482 (1962).
- R. H. Brooks and A. T. Corey, "Properties of porous media affecting fluid flow," *J. Irrig. Drain. Div.* **92**(2), 61 (1966).
- M. T. van Genuchten, "A closed-form equation for predicting the hydraulic conductivity of unsaturated soils," *Soil Sci. Soc. Am. J.* **44**, 892 (1980).
- O. C. Zienkiewicz and T. Shiomi, "Dynamic behavior of saturated porous media: The generalized Biot formulation and its numerical solution," *Int. J. Numer. Anal. Methods Geomech.* **8**, 71 (1984).
- H. H. Liu, J. Rutqvist, and J. G. Berryman, "On the relationship between stress and elastic strain for porous and fractured rock," *Int. J. Rock. Mech. Min. Sci.* **46**(2), 289 (2009).
- S. A. Moosavi, K. Goshtasbi, E. Kazemzadeh *et al.*, "Relationship between porosity and permeability with stress using pore volume compressibility characteristic of reservoir rocks," *Arab. J. Geosci.* **7**(1), 231 (2014).
- J. T. Zheng, L. G. Zheng, H. H. Liu, and Y. Ju, "Relationships between permeability, porosity and effective stress for low-permeability sedimentary rock," *Int. J. Rock. Mech. Min. Sci.* **78**, 304 (2015).
- L. Y. Chin, R. Rajagopal, and L. K. Thomas, "Fully coupled geomechanics and fluid-flow analysis of wells with stress-dependent permeability," *SPE J.* **5**(1), 32 (2000).
- M. Gutierrez, R. W. Lewis, and I. Masters, "Petroleum reservoir simulation coupling fluid flow and geomechanics," *SPE Reservoir Eval. Eng.* **4**(3), 164 (2001).
- J. Q. Shi and S. Durucan, "Drawdown induced changes in permeability of coalbeds: A new interpretation of the reservoir response to primary recovery," *Transp. Porous Media* **56**, 1–16 (2004).
- R. Nair, Y. Aboaleiman, and M. Zaman, "Modeling fully coupled oil-gas flow in a dual-porosity medium," *Int. J. Geomech.* **5**, 326 (2005).
- T. R. Ma, J. Rutqvist, C. M. Oldenburg *et al.*, "Fully coupled two-phase flow and poromechanics modeling of coalbed methane recovery: Impact of geomechanics on production rate," *J. Nat. Gas Sci. Eng.* **45**, 474 (2017).
- Y. Z. Liu, L. J. Liu, J. Y. Leung, and G. J. Moridis, "Sequentially coupled flow and geomechanical simulation with a discrete fracture model for analyzing fracturing fluid recovery and distribution in fractured ultra-low permeability gas reservoirs," *J. Pet. Sci. Eng.* **189**, 107042 (2020).
- A. Sangnimnuan, J. W. Li, and K. Wu, "Development of coupled two phase flow and geomechanics model to predict stress evolution in unconventional reservoirs with complex fracture geometry," *J. Pet. Sci. Eng.* **196**, 108072 (2021).
- J. Kim, E. L. Sonnenthal, and J. Rutqvist, "Formulation and sequential numerical algorithms of coupled fluid/heat flow and geomechanics for multiple porosity materials," *Int. J. Numer. Methods Eng.* **92**(5), 425 (2012).
- W.-j. Shen, X.-h. Liu, X.-z. Li, and J.-l. Lu, "Investigation of water coning mechanism in Tarim fractured sandstone gas reservoirs," *J. Cent. South Univ.* **22**(1), 344 (2015).
- Y. S. Wu, "Numerical simulation of single-phase and multiphase non-Darcy flow in porous and fractured reservoir," *Transp. Porous Media* **49**(2), 209 (2002).
- M. Bai, D. Elsworth, and J. C. Roegiers, "Multiporosity/multipermeability approach to the simulation of naturally fractured reservoirs," *Water Resour. Res.* **29**(6), 1621–1633, <https://doi.org/10.1029/92WR02746> (1993).
- B. C. Yan, M. Alf, C. An *et al.*, "General multi-porosity simulation for fractured reservoir modeling," *J. Nat. Gas Sci. Eng.* **33**, 777–791 (2016).
- J. Rutqvist, L. Börgessonb, M. Chijimatsuc *et al.*, "Thermohydromechanics of partially saturated geological media: Governing equations and formulation of four finite element models," *Int. J. Rock Mech. Min. Sci.* **38**, 105 (2001).
- F. Pesavento, D. Gawin, and B. A. Schrefler, "Modeling cementitious materials as multiphase porous media: Theoretical framework and applications," *Acta Mech.* **201**(1–4), 313 (2008).
- M. A. Bagheri and A. Settari, "Modeling of geomechanics in naturally fractured reservoirs," *SPE Reservoir Eval. Eng.* **11**(1), 108 (2008).
- R. Yang, T. R. Ma, H. Xu *et al.*, "A model of fully coupled two-phase flow and coal deformation under dynamic diffusion for coalbed methane extraction," *J. Nat. Gas Sci. Eng.* **72**, 103010 (2019).
- H. Shi, X. R. Luo, H. J. Yang *et al.*, "Sources of quartz grains influencing quartz cementation and reservoir quality in ultra-deeply buried sandstones in Keshen-2 gas field, north-west China," *Mar. Pet. Geol.* **98**, 185 (2018).
- J. C. Wang, L. Zhao, X. Z. Zhang *et al.*, "Natural fracture opening preservation and reactivation in deep sandstones of the Kuqa foreland thrust belt, Tarim Basin," *Mar. Pet. Geol.* **127**, 104956 (2021).
- X. S. Lu, M. J. Zhao, K. Y. Liu *et al.*, "Formation condition of deep gas reservoirs in tight sandstones in Kuqa Foreland Basin," *Pet. Res.* **3**, 346 (2018).
- W. J. Shen, Y. M. Xu, and X. Z. Li, "Numerical simulation of gas and water flow mechanism in hydraulically fractured shale gas reservoirs," *J. Nat. Gas Sci. Eng.* **35**, 726 (2016).
- X. Z. Li, D. T. Lu, R. L. Luo, Y. P. Sun *et al.*, "Quantitative criteria for identifying main flow channels in complex porous media," *Pet. Explor. Dev.* **46**(5), 998 (2019).
- J. J. Ijeje, Q. Gan, and J. C. Cai, "Influence of permeability anisotropy on heat transfer and permeability evolution in geothermal reservoir," *Adv. Geo-Energy Res.* **3**(1), 43–51 (2019).

- ⁴²J. C. Jiao, Y. Hu, X. Xu *et al.*, “Study on the effects of fracture on permeability with pore-fracture network model,” *Energy Explor. Exploit.* **36**(6), 1556 (2018).
- ⁴³Z. P. Meng, J. C. Zhang, and R. Wang, “In-situ stress, pore pressure and stress-dependent permeability in the Southern Qinshui Basin,” *Int. J. Rock. Mech. Min. Sci.* **48**(1), 122 (2011).
- ⁴⁴M. C. Villeneuve, M. J. Heap, A. R. L. Kushnir *et al.*, “Estimating in situ rock mass strength and elastic modulus of granite from the Soultz-sous-Forêts geothermal reservoir (France),” *Geotherm. Energy* **6**, 11 (2018).
- ⁴⁵Q. Wang and S. C. Ji, “Poisson’s ratios of crystalline rocks as a function of hydrostatic confining pressure,” *J. Geophys. Res.: Solid Earth* **114**, B09202, <https://doi.org/10.1029/2008JB006167> (2009).